J. Plasma Physics (2009), *vol.* 75, *part* 4, *pp.* 437–454.
doi:10.1017/S0022377809008137 Printed in the United Kingdom

A length-scale formula for confined quasi-two-dimensional plasmas

TIMOTHY D. ANDERSEN and CHJAN C. LIM

Mathematical Sciences, RPI, 110 8th Street, Troy, NY 12180, USA
(andert@alum.rpi.edu)

(Received 5 June 2008, revised 29 September 2008 and accepted 10 October 2008, first published online 1 June 2009)

Abstract. Typically a magnetohydrodynamical model for neutral plasmas must take into account both the ionic and the electron fluids and their interaction. However, at short time scales, the ionic fluid appears to be stationary compared to the electron fluid. On these scales, we need consider only the electron motion and associated field dynamics, and a single fluid model called the electron magnetohydrodynamical model which treats the ionic fluid as a uniform neutralizing background applies. Using Maxwell's equations, the vorticity of the electron fluid and the magnetic field can be combined to give a generalized vorticity field, and one can show that Euler's equations govern its behavior. When the vorticity is concentrated into slender, periodic, and nearly parallel (but slightly three-dimensional) filaments, one can also show that Euler's equations simplify into a Hamiltonian system and treat the system in statistical equilibrium, where the filaments act as interacting particles. In this paper, we show that, under a mean-field approximation, as the number of filaments becomes infinite (with appropriate scaling to keep the vorticity constant) and given that angular momentum is conserved, the statistical length scale, R, of this system in the Gibbs canonical ensemble follows an explicit formula, which we derive. This formula shows how the most critical statistic of an electron plasma of this type, its size, varies with angular momentum, kinetic energy, and filament elasticity (a measure of the interior structure of each filament) and in particular it shows how three-dimensional effects cause significant increases in the system size from a perfectly parallel, two-dimensional, one-component Coulomb gas.

1. Introduction

Plasma confinement is critical to magnetic nuclear fusion. Given a neutral plasma in a strongly confining magnetic field, columns of electrons and ions align, and the plasma behaves as a two-dimensional (2D) fluid. However, one of the great obstacles to confinement comes from the increasing impact of three-dimensional (3D) effects, defects in the alignment of columns due to fluctuations, as the plasma is further confined (Figures 1 and 2). 2D models are insufficient to deal with this problem and, in statistical equilibrium, fail to accurately predict the length scale of dense plasmas in the unbounded plane under conservation of angular momentum.

Because of its mathematical simplicity and apparent applicability to highly aligned magnetically confined plasmas (and other Euler fluids), 2D fluid models such as Onsager's point vortex gas [1] have dominated the statistical equilibrium

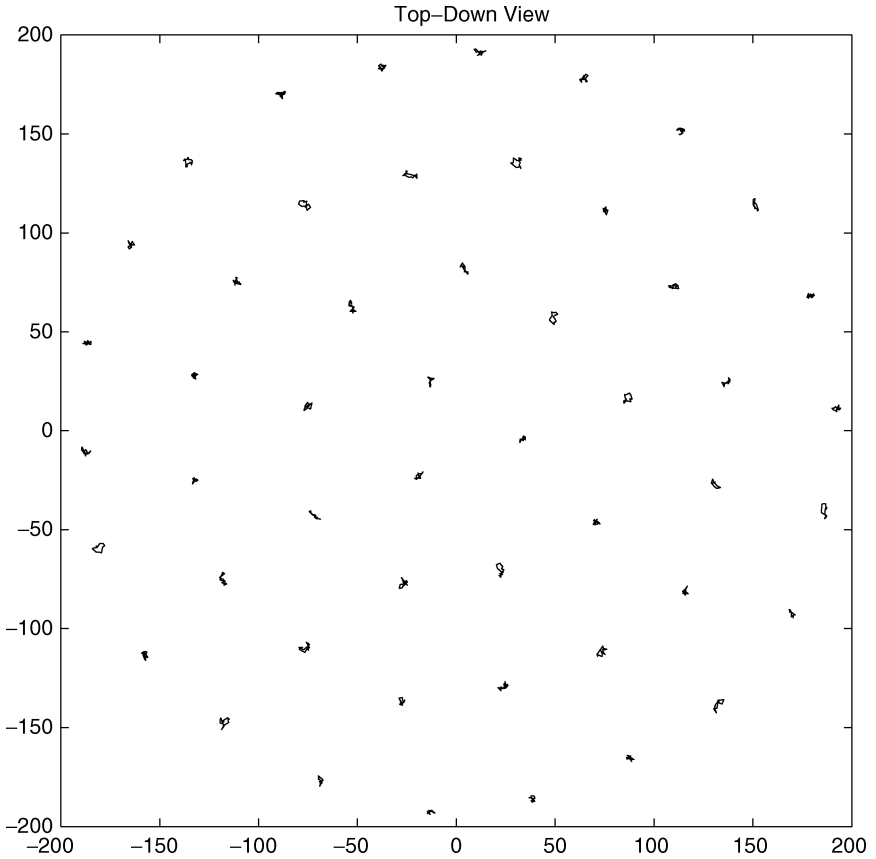

Figure 1. Shown here in top-down projection are nearly parallel vortex filaments, at low density and high strength of interaction, well ordered into a 2D triangular lattice known as the Abrikosov lattice from type-II superconductors [24]. This figure (taken from a single Monte Carlo sample) shows how the quasi-2D model is essentially a 2D model for these parameters.

approach to plasmas and other fluids for decades. The literature on the point vortex gas and its relatives is quite extensive. Seminal papers such as Onsager's and Joyce and Montgomery [2] and Edwards and Taylor [3] describe negative-temperature states in fluids and guiding center plasmas (where temperature is virtual, treating vortices as if they were molecules rather than collections of them). Mathematical rigor has been applied in the form of existence proofs for the asymptotic mean-field approach to this 2D problem in Caglioti et al. [4], Kiessling [5], and Kiessling and Spohn [6]. (For a more complete overview, see Lim [7] and Lim and Nebus [8].) 2D models work well for plasmas that are not well confined (sparse), but they ignore the internal entropy of the filaments – their 'unwillingness' to remain aligned even under strong confinement. This entropy creates 3D effects that become noticeable when the confining field brings filaments close together.

Theoretical derivations for 3D fluids are difficult and tend to focus on single columns [9, 10, 11, 12]. In 1995, Uby et al. [13] described the dynamics of the combined magnetic and vorticity field (known as a generalized vorticity field) of a single filament of electrons in a neutral plasma using the short time scale electron magnetohydrodynamical (EMH) model. Earlier, Kinney et al. [14] had

https://doi.org/10.1017/S0022377809008137 Published online by Cambridge University Press

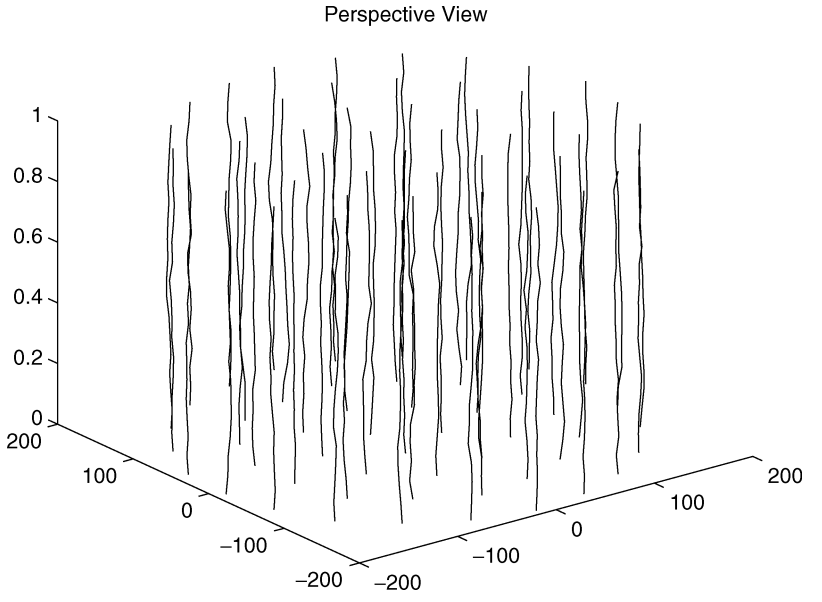

Figure 2. Nearly parallel vortex filaments are nearly parallel to the z axis in an asymptotic sense that their deviation from straightness is a small parameter. They are infinite in length but have a period L. Here there are 50 filaments.

used this same model to describe the interaction of a system of perfectly parallel (2D) filaments of generalized vorticity (an alternative to the guiding center 2D approach to plasmas but mathematically equivalent), suggesting that the two approaches could be combined into a system of interacting, slightly 3D, nearly parallel filaments of generalized vorticity such as Klein et al. [15] have done for Navier–Stokes fluids. At the same time, several authors including Weinan [16] have considered the dynamics of vorticity in the context of superconductivity and superfluids.

This nearly parallel electron vorticity model provides a platform from which to investigate the relatively unknown impact of 3D effects on large-scale, short-duration structures in confined plasmas.

The EMH model is a simplification of the two-fluid magnetohydrodynamical model. As time intervals become small, the ionic fluid appears stationary and its behavior can be treated as a neutralizing background. In this model, the magnetic field, $\mathbf{B} = \nabla \times \mathbf{A}$, and the charged fluid vorticity, $\boldsymbol{\omega} = \nabla \times \mathbf{v}$, combine into a general vorticity field, $\Omega = \nabla \times \mathbf{p}$, where the generalized momentum $\mathbf{p} = m\mathbf{v} - e\mathbf{A}$; m is the electron mass, $-e$ is the electron charge, $\mathbf{v}$ is the fluid velocity field, and $\mathbf{A}$ is the magnetic vector potential field. For a brief overview of the model, see Uby et al. [13]. A detailed model discussion can be found in Gordeev et al. [17].

In the case of dense turbulent plasmas, a statistical approach is preferable to direct numerical PDE (Partial Differential Equation) simulations because of the large number of dimensions (in the thousands). Given that we assume that the generalized vorticity field takes the form of nearly parallel slender filaments with appropriate asymptotic constraints (described below), the EMH model describes a Hamiltonian system. Even though the model is for short time scales, this Hamiltonian system can be studied in a statistical equilibrium ensemble with the caveat

that the macroscopic coherent structures self-organize over a relaxation time scale that is short compared to the dissipation time scale.

For an analogous example, consider the large vortex that forms from initially swirling tea in a cup – a case of freely decaying quasi-2D turbulence [18]. While this vorticity does not last long, it can be properly treated as the statistical equilibrium result [19], where the time scale for the inverse cascade of energy to large spatial scales is much shorter than the Ekman dissipation time scale. Moreover, over short durations energy dissipation in the interior of the flow can be ignored because the viscous dissipation time scale is much longer than the Ekman dissipation time scale. Of course, without energy dissipation, either in the interior of the flow or in the Ekman boundary layers, the tea would swirl forever. A more rigorous approach is discussed in [20], where it is shown that systems not in thermal equilibrium and irreversible systems can often undergo symmetry-breaking phase transitions and self-organize like their counterparts in equilibrium.

The same is true for confined plasmas, and we are particularly interested in short-duration structures and how they interfere with attaining sufficient confinement for fusion. What remains is to choose an appropriate statistical model.

Two statistical equilibrium ensembles are applicable to this problem: (1) the canonical in which we assume that the system is not in isolation and that energy can be exchanged with an exterior medium and (2) the microcanonical where the system is isolated and energy and angular momentum are absolutely conserved. The microcanonical ensemble would model a plasma experiencing no outside influence. In a tokamak, this would imply that the magnetic confinement is shut off. The canonical ensemble describes the case where energy is allowed to pass between the plasma and the magnetic field (effectively an infinite reservoir). In a previous paper we considered the microcanonical ensemble [21]. Here we address the problem of when there is an energy/angular momentum exchange medium surrounding the system, i.e. the canonical ensemble.

Because of the difficulty in calculating partition functions (and thus solving the ensemble exactly), we focus on calculating an individual moment. The primary moment for any system that is translation invariant and on the unbounded plane is the second moment, essentially size. The size of the system gives us the most intuitive idea of how the system is behaving and, for confined plasmas, it gives us a good idea of how easy it is to squeeze the plasma magnetically. Lim and Assad [22] have calculated the second moment of the canonical guiding center plasma, giving an explicit formula for low temperature in the mean-field limit. The formula for the nearly parallel system in the same limit (if it exists in explicit form) has never been calculated.

In this paper, we calculate a novel explicit formula for the size (second moment) of the system of nearly parallel generalized vorticity filaments with conserved angular momentum. This formula comes from a free energy minimization derived from the Gibbs canonical ensemble using the rigorous mean-field theory of Lions and Majda [23]. We validate this formula with path-integral Monte Carlo (PIMC) simulations. Our formula and Monte Carlo results agree well and both indicate that 3D effects become significant at a particular density. We show that at high densities point vortices and nearly parallel vortex filaments have qualitatively different behavior. While the size of the point vortex plasma collapses with increasing temperature [22], nearly parallel filaments, which at low density behave exactly like point vortices, reverse their collapse, causing expansion (Sec. 6). We

hypothesize that this reversal arises from the additional entropy of the system present in individual filaments.

2. Background

2.1. Equations of motion

We derive the standard EMH equations of motion in the manner of Uby et al. [13].

For an electron fluid (neglecting collisions with the neutralizing background),

$$m\left[\frac{\partial \mathbf{v}}{\partial t}\right] = \frac{-\nabla P}{n} - e(\mathbf{E} + \mathbf{v} \times \mathbf{B}), \tag{1}$$

where m and $-e$ are the electron mass and charge; $\mathbf{v}$, n, and P are electron fluid velocity, number density, and pressure. When electron displacement current is neglected, Ampère's law for the magnetic field gives

$$\nabla \times \mathbf{B} = -\mu_0 e n \mathbf{v}, \tag{2}$$

and Faraday's law determines the electric field $\mathbf{E}$.

Given that the pressure is a function of number density and the fluid is incompressible, taking the curl of (1),

$$\frac{\partial \mathbf{\Omega}}{\partial t} = \nabla \times (\mathbf{v} \times \mathbf{\Omega}), \tag{3}$$

where $\mathbf{\Omega} = \nabla \times \mathbf{p}$ is generalized vorticity and $\mathbf{p} = m\mathbf{v} - e\mathbf{A}$ generalized momentum.

Combining (2) with the frozen-field equation, (3), we have

$$\mathbf{\Omega} = -e[\mathbf{B} + \nabla \times (\lambda^2 \nabla \times \mathbf{B})], \tag{4}$$

where $\lambda = c/\omega_{\mathrm{pe}}$ is the penetration depth. The electron plasma frequency is $\omega_{\mathrm{pe}}^2 = ne^2/m\varepsilon_0$.

For a homogeneous plasma,

$$\mathbf{\Omega} = \mathbf{B} - \lambda^2 \nabla^2 \mathbf{B}, \tag{5}$$

where the magnetic field and generalized vorticity have been scaled: $-e\mathbf{B}/m \to \mathbf{B}$ and $\mathbf{\Omega}/m \to \mathbf{\Omega}$. Equation (2) becomes $\mathbf{v} = \lambda^2 \nabla \times \mathbf{B}$ and along with (3) and (5) describes the motion of the electron fluid.

Equation (3) has the same form as the vorticity equation for ordinary fluids from which Lions and Majda [23] derived the nonlinear Schrödinger PDE and Hamiltonian equations for the system of nearly parallel filaments in this paper.

The stability of vortices with respect to short-wave perturbations is shown in Ivonin [25].

2.2. Gibbs canonical ensemble

In formal notation, a canonical Gibbs' measure has that if a state s has energy E_s and angular momentum M_s, then the probability of s is

$$P(E_s, I_s) \propto e^{-\beta E_s - \mu M_s}, \tag{6}$$

where β and μ are constants. Since $\sum_s P(E_s, M_s) = 1$, $P(E_s, M_s) = Z^{-1} e^{-\beta E_s - \mu M_s}$, where $Z = \sum_s e^{-\beta E_s - \mu M_s}$ [19]. Alternatively, we can let $p = \mu/\beta$ be constant (for plasmas, the Larmor frequency) and enthalpy be $H_s = E_s + pM_s$, in which case we have an ensemble in a single conserved quantity: $P(H_s) = Z^{-1} \exp(-\beta H_s)$.

https://doi.org/10.1017/S0022377809008137 Published online by Cambridge University Press

For historical reasons β is known as inverse 'temperature' although it is not directly related to its molecular equivalent because the 'molecules' here are vortices. The multiplier μ reflects the relationship between the angular momentum and the energy and μ/β is the Larmor frequency ($\omega_{\texttt{Larmor}}$) [22] and can be thought of as a 'pressure' term defining how squeezed the system is. Because β has units of inverse energy and μ has units of frequency over energy and μ/β has units of inverse time or frequency.

There is little in the literature to say what β is or how to measure it, although it does have a well-defined meaning. The temperature of a microcanonical system is well defined as $1/T_{\rm mc} = dS(E,N)/dE$, the rate of increase of entropy with energy where the microcanonical entropy $S(E,N)$ is given by the natural logarithm of the microcanonical partition function $Z_{\rm mc}(E,N)$. One way to calculate the canonical inverse temperature β is to invoke a large-deviation result that holds even in the case that the Gibbs (canonical) measure is weakly inequivalent to the microcanonical ensemble, that is, the Gibbs measure or canonical partition function $Z_{\rm c}(\beta,N)$ is overwhelmingly concentrated at the most-probable macrostate, for which the relationship $\beta = dS(E,N)/dE$ holds. In this case, the definitions of temperature in the canonical and microcanonical formulations are in agreement, even though the two ensembles are not strictly equivalent – for example, this weak inequivalence allows the specific heat in the microcanonical ensemble to take on negative values whilst its canonical counterpart must be positive. This extends to weakly inequivalent ensembles; the standard inverse procedure for determining canonical temperature as a function of the fixed energy level E in the microcanonical ensemble is through the relationship $\langle E\rangle_{\rm c}(T(E)) = E$, where the subscript c denotes the canonical average.

In the EMH model, β is precisely related to the kinetic energies associated with the macroscopic motions (flows) and magnetic fields in the plasma, and thus to the total generalized vorticity, $\int d^3x\,\Omega(x,y,z)$.

2.3. Length scale for point vortex equilibrium statistics

The low-temperature (asymptotic as $\beta \to \infty$) statistics of strictly 2D point vortices, guiding center plasmas, and 2D EMH generalized vorticity in the unbounded plane with angular momentum conserved are well understood [7]. The point vortex gas model has the energy functional

$$E_N^{\rm 2D} = -\sum_{j>i} \lambda_i \lambda_j \log|\Psi_i - \Psi_j|^2, \tag{7}$$

where λ_i and λ_j are the circulation constants for point vortices i and j and Ψ_i and Ψ_j are their positions in the complex plane. This Hamiltonian derives from the 2D Euler equations in vorticity form given that ω, the field, has the form

$$\omega(\Psi) = -\sum_j \lambda_j \delta(\Psi - \Psi_j),$$

where Ψ is a position in the complex plane [19].

In their paper, Lim and Assad [22] showed variationally that the mean-square vortex position (variance) for 2D point vortices,

$$R_{\rm 2D}^2 = \left\langle N^{-1} \sum_i |\Psi_i|^2 \right\rangle, \tag{8}$$

https://doi.org/10.1017/S0022377809008137 Published online by Cambridge University Press

has a formula as $N \to \infty$. If $\Omega = \sum_i \lambda_i$ is the total circulation and we let $\lambda_i = \Omega/N$, then taking the limit on the Gibbs canonical ensemble, we have the non-dimensional variance,

$$R_{2\mathrm{D}}^2 = \frac{\Omega\beta}{4\mu}. \tag{9}$$

In Monte Carlo simulations of an ensemble of 1000 point vortices, Assad and Lim [26] showed that the distribution of vortices is almost uniform and axisymmetric, meaning that the probability distribution of vortices is nearly a perfect cylinder, suggesting that $R_{2\mathrm{D}}^2$ is the only valuable statistic.

3. The nearly parallel vortex filament model

We define nearly parallel vortex filaments as in [15].

Nearly parallel vortex filaments are $C^2([0, L])$ curves that we can represent with a complex parametrization $\Psi_i(\tau)$, where $\Psi_i(\tau) = x_i(\tau) + iy_i(\tau)$ and $\tau \in [0, L)$. They have a special asymptotic form. Given that $L \in O(1)$, if we take any two values of τ, τ_0, and τ_1 such that $\tau_0 < \tau_1$, and let $\Delta\tau = \tau_1 - \tau_0$ such that $\Delta\tau \in O(\varepsilon)$, where $\varepsilon \ll 1$, then for any filament i, the amplitude $|\Psi_i(\tau_1) - \Psi_i(\tau_0)| \in O(\varepsilon^2)$. In words this means that, for a small rise of length ε in the filament, the amplitude must be on the order of ε^2. This assumption guarantees a certain degree of straightness in the filament that allows for the derivation of the quasi-2D equations of motion. The other asymptotic assumption is of the vortex core size, h, which has the property $h \ll \varepsilon$. In this model we assume that the vortices have no cross section, i.e. the vorticity field, ω, has the form

$$\omega = \sum_i \delta(\Psi(\tau) - \Psi_i(\tau)), \tag{10}$$

where $\Psi(\tau) = x(\tau) + iy(\tau)$ corresponds to the 3D Cartesian position $(x(\tau), y(\tau), \tau)$.

Combining the energy functionals of Kinney et al. [14] and Uby et al. [13], we have

$$E_N = \alpha \int_0^L d\tau \sum_{i=1}^{N} \frac{1}{2}\left|\frac{\partial\Psi_i(\tau)}{\partial\tau}\right|^2 - \int_0^L d\tau \sum_{i=1}^{N}\sum_{j>i}^{N} \log|\Psi_i(\tau) - \Psi_j(\tau)|, \tag{11}$$

where α is the core-elasticity constant in units of energy/length and results from an asymptotic matching procedure [11, 13]. This functional resembles the 2D point vortex energy in that the interaction is logarithmic in the plane. For two filaments i and j, only points in the same plane, the same value of τ, interact. Two points at different values of τ only interact if they are both on the same filament. The first term is a local self-induction term that causes the filaments to bend. The additional conserved quantity, angular momentum, is given by

$$M_N = \sum_i \int_0^L d\tau\, |\Psi_i(\tau)|^2, \tag{12}$$

with the assumption that the magnetic field **B** is uniform and axisymmetric, centered around the central axis. The angular momentum is not generalized, however, because, as is well known, an external magnetic field cannot influence equilibrium statistics. Therefore, M_N is only angular momentum and contains none of the magnetic moment.

https://doi.org/10.1017/S0022377809008137 Published online by Cambridge University Press

Lions and Majda [23] introduced a broken-segment model in Sec. 2.2, Equation (2.20) of their paper. For each i, $\Psi_i(\tau)$ is piecewise linear with M segments. Each vertex or 'bead' is at a multiple of $\epsilon = L/M$. Therefore, we define $\psi_i(k) = \Psi_i((k-1)\epsilon)$, and the curve for filament i is given by the vector $\Psi_i = (\psi_i(1), \ldots, \psi_i(M))$. With this representation, we rewrite the conserved quantities

$$E_N(M) = \alpha \sum_{i=1}^{N} \sum_{k=1}^{M} \frac{1}{2} \frac{|\psi_i(k+1) - \psi_i(k)|^2}{\epsilon} - \sum_{i=1}^{N} \sum_{j>i}^{N} \sum_{k=1}^{M} \epsilon \log |\psi_i(k) - \psi_j(k)|, \tag{13}$$

$$M_N(M) = \sum_{i=1}^{N} \sum_{k=1}^{M} \epsilon |\psi_i(k)|^2. \tag{14}$$

The Gibbs probability measure for a state $s = (\Psi_1, \ldots, \Psi_N)$ is then

$$P(s) = Z^{-1} \exp(-\beta E_N(M) - \mu M_N(M)), \tag{15}$$

where the partition function has the form

$$Z_N(M) = \int_{\mathscr{C}^{M\,N}} d\Psi_1 \cdots d\Psi_N \exp(-\beta E_N(M) - \mu M_N(M)). \tag{16}$$

Note that a careful choice of parameters β, μ, etc. causes any non-nearly-parallel states to have such large energies that their probabilities are negligible. For such parameter ranges, we can assume that the Gibbs canonical model is physical. Our Monte Carlo simulation naturally rejects states with non-nearly-parallel lines.

We note that while it is possible to simulate the system with Monte Carlo it is not possible to solve explicitly for Z_N for any given value of M. In their paper, Lions and Majda [23] go on to derive a nonlinear Schrödinger equation that can give approximate values for $P(s)$. Their PDE captures a great deal of the statistics, but they do not provide any explicit formula for the length scale R, which is our goal. We refer the reader to their paper to learn more about their derivation and the model.

4. Free energy theory

4.1. Free energy of most-probable macrostate

Given a functional for the free energy for a system, F, it is possible to solve for the statistics of the most-probable macrostate by minimizing F with respect to the desired statistic. In our case the statistic is defined as the mean-square vortex position for a given number of filaments N,

$$R^2 = \left\langle (LN)^{-1} \sum_{i=1}^{N} \int_0^L d\tau \, |\Psi_i(\tau)|^2 \right\rangle, \tag{17}$$

where $\Psi_i(\tau) = x_i(\tau) + iy_i(\tau)$ is a complex number representing the 2D position of filament i at $z = \tau$ and the average $\langle * \rangle$ is with respect to the 3D Gibbs probability measure in Ψ_i, $P_N = Z_N^{-1} \int d\Psi_1 \cdots d\Psi_N \exp(-\beta E_N - \mu M_N)$, where E_N is defined by (11) and M_N by (12).

In our system we write the free energy as follows:

$$F_N = \langle E_N \rangle + \frac{\mu}{\beta} \langle M_N \rangle - \frac{1}{\beta} S_N, \tag{18}$$

https://doi.org/10.1017/S0022377809008137 Published online by Cambridge University Press

where S_N is the entropy and $\langle E_N \rangle + (\mu/\beta)\langle M_N \rangle$ is the total enthalpy. Temperature $T = 1/\beta$.

The function Z_N can be considered a sum over microstates, s_i, or it can be an average over a set of macrostates, σ_j. Equation (16) is a sum over microstates. Alternatively, the partition function is given by the formula

$$Z_N = \sum_j \exp(-\beta E_N[\sigma_j] - \mu M_N[\sigma_j]) P[\sigma_j], \tag{19}$$

where E_N is the energy, M_N is the angular momentum, and P is the probability for macrostate σ_j.

Since $S_N[\sigma_j] = \log P[\sigma_j]$, using (18), we can say that

$$\begin{aligned} Z_N &= \sum_j \exp(-\beta E_N[\sigma_j] - \mu M_N[\sigma_j] + S[\sigma_j]) \\ &= \sum_j \exp(-\beta F_N[\sigma_j]). \end{aligned} \tag{20}$$

Because of conservation laws, we assume in physics that the most-probable macrostate or energy state, $j = \mathrm{m}$, has a probability so much larger than the probabilities of all other macrostates that sum contributions from other macrostates can be neglected and

$$Z_N = \exp(-\beta F_N[\sigma_\mathrm{m}]). \tag{21}$$

Therefore, we have an equation for the free energy,

$$F_N = -\frac{1}{\beta} \log Z_N. \tag{22}$$

Even though this free energy is only the free energy of the most-probable macrostate, it can be considered the system's free energy.

As mentioned in Sec. 3, we cannot solve for Z_N. We need to approximate it to derive the free energy functional. One way to do this is with a mean-field theory.

4.2. Mean-field theory

In Lions and Majda [23], they developed a mean-field PDE that describes the probability distribution of the filaments in top-down projection. One of the solutions to that PDE is a uniform distribution which is exact in the limit as $\beta \to \infty$ (low temperature) and $N \to \infty$, given appropriate scaling of other parameters to avoid a blow up of the energy functional. The uniform distribution is over a cylinder of radius $2R$ and height L. It causes the interaction energy and angular momentum to become constants and imposes a 'spherical constraint' on the integral. We include this constraint as a microcanonical or exact constraint into the partition function,

$$Z'_N(M) = \left\{ \int d\Psi \, e^{(-\beta E(M) - \mu M R^2)} \delta\left(R^2 - \sum_{k=1}^{M} M^{-1} |\psi(k)|^2 \right) \right\}^N, \tag{23}$$

where

$$E(M) = \alpha \sum_{k=1}^{M} \frac{1}{2} \frac{|\psi_i(k+1) - \psi_i(k)|^2}{\epsilon} - N \Big/ 4 \sum_{k=1}^{M} \epsilon \log R^2. \tag{24}$$

https://doi.org/10.1017/S0022377809008137 Published online by Cambridge University Press

Note that the sum over N has become a power because the iterated integrals have separated into a product of integrals with the disappearance of the interdependences in the interaction term.

This constraint eliminates fluctuations in interaction energy and angular momentum (as the limit in β of the mean-field theory implies), leaving only fluctuations in local self-induction energy. This elimination provides the best opportunity for comparison with the 2D length-scale work of [22] that also eliminates these two types of fluctuation.

4.3. Spherical model solution

Equation (23) is a multidimensional Gaussian integral with a spherical constraint – so called because it forces the vector Ψ to stay on the $(M-1)$-sphere of radius $\sqrt{M}R$. To evaluate it we turn to the spherical model of [27]. The spherical model was first used in fluid mechanics in an energy–entropy theory for transitions to super-rotation in barotropic flows coupled to massive rotating spheres [8].

The spherical model comprises a number of steps for evaluating integrals of the form (23), beginning by putting the Dirac delta function into integral form and ending with a steepest descent evaluation of the integral over Ψ.

In integral (Fourier) form the Dirac delta reads

$$\delta\left(MR^2 - \sum_{k=1}^{M} |\psi(k)|^2\right) = \int_{-\infty}^{\infty} \frac{d\sigma}{2\pi} \exp\left[-i\sigma\left(MR^2 - \sum_{k=1}^{M} |\psi(k)|^2\right)\right], \tag{25}$$

and allows us to combine the function in the exponent in (23) with the exponent of the spherical constraint. (Whereas before σ was used as a symbol for a macrostate, here it is an integration variable.)

4.4. Free energy derivation for R

Now we can determine the free energy functional, which ought to be minimal under the constraints of the system, via steepest descent. Determining the free energy as a function of the particular statistic, R, is more useful than having an equation for the partition function itself because we can determine R by minimizing the free energy with respect to it and then solving for R.

Given the partition function defined in (23) and the free energy in (18), as $M, N \to \infty$, the value for R^2, defined in (17), for the minimal free energy is

$$R^2 = \frac{\beta'^2\alpha' + \sqrt{\beta'^4\alpha'^2 + 32\alpha'\beta'\mu}}{8\alpha'\beta'\mu}, \tag{26}$$

where $\alpha' = \alpha/N$ and $\beta' = \beta N$ are scaled non-extensively. The proof of this result is given in Appendix A, and we drop primes henceforth.

The resulting expression for the square length scale R^2 is useful for comparison with the length-scale result of Lim and Assad [22] because, if we take the limit

$$\lim_{\alpha\to\infty} \frac{\beta^2\alpha + \sqrt{\beta^4\alpha^2 + 32\alpha\beta\mu}}{8\alpha\beta\mu} = \frac{\beta}{4\mu}, \tag{27}$$

we get back the 2D point vortex result for the length scale, which shows that our formula and the Lim and Assad [22] formula agree for perfectly straight filaments.

However, for finite α the two formulae show a significant difference. The 2D formula is linear in β; our formula is nonlinear. In fact, for decreasing β, the sign

https://doi.org/10.1017/S0022377809008137 Published online by Cambridge University Press

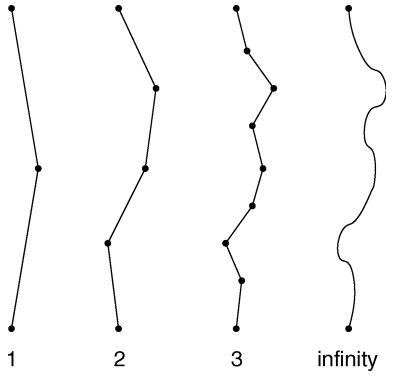

Figure 3. The bisection algorithm works by bisecting the filament to sample point positions. First the center point is selected, then the two points half-way from the center to the end points, then four more points, eight, and so on until some maximum number of points are sampled. These are snapshots of one filament at different steps in the sampling process.

of the slope of our formula changes at $\beta = \beta_0$, where

$$\beta_0^3 = \frac{4\mu}{\alpha}. \tag{28}$$

That the system collapses and then starts to expand as 'temperature', $1/\beta$, increases indicates a significant departure from the strictly 2D where the system size only collapses. In Sec. 6, we show that Monte Carlo Simulations confirm this result and that the straightness assumptions of the model hold through much of the expansion phase.

5. Monte Carlo

Path-integral Monte Carlo Simulations methods emerged from the path-integral formulation invented by Dirac that Richard Feynman later expanded [28], in which particles are conceived to follow all paths through space. One of Feynman's great contributions to the quantum many-body problem was the mapping of path integrals onto a classical system of interacting 'polymers' [29]. Ceperley used Feynman's convenient piecewise-linear formulation to develop his PIMC method which he successfully applied to He-4, generating the well-known lambda transition for the first time in a microscopic particle simulation [30]. Because it describes a system of interacting polymers, the PIMC method applies to classical systems that have a 'polymer'-type description like nearly parallel vortex filaments.

The PIMC method has several advantages. It is a *continuum* Monte Carlo algorithm, relying on no spatial lattice. Only time (length in the z direction in the case of vortex filaments) is discretized, and the algorithm makes no assumptions about types of phase transitions or trial wavefunctions.

The Monte Carlo simulation begins with a random distribution of filament end points in a square of side 10, and there are two possible moves that the algorithm chooses at random.

(a) It moves a filament's end points, $\psi_i(1)$ and $\psi_i(M+1)$. The index i is chosen at random, and filament i's end points are moved a uniform random distance.

(b) It keeps end points stationary and, following the bisection method of Ceperley (Fig. 3), grows a new internal configuration for a randomly chosen filament [30].

https://doi.org/10.1017/S0022377809008137 Published online by Cambridge University Press

In each case, the energy of the new state, s', is calculated and retained with probability

$$A(s \to s') = \min\{1, \exp(-\beta[E_N^{s'}(M) - E_N^s(M)] - \mu[M_N^{s'}(M) - M_N^s(M)])\}, \quad (29)$$

where s is the previous state. This effectively samples states from the Gibbs probability distribution in (15).

Our stopping criterion is graphical in that we ensure that the cumulative arithmetic mean of the energy,

$$E_{\text{cum}}^k = k^{-1} \sum_{i=1}^{k} E_N(s_i) + \frac{\mu}{\beta} M_N(s_i), \quad (30)$$

where s_i refers to the state resulting from the ith move and k is the current move index, settles to a constant. The energy is almost guaranteed to settle in the case of the Gibbs' measure because of the tendency for the system to select a particular energy state (mean energy) and remain close to that state. Typically, we run for 1 million moves (accepted plus rejected) or 50 000 sweeps for 20 vortices. Afterwards, we collect data from about 200 000 moves (1000 sweeps) to generate statistical information.

6. Results

6.1. Comparison

We simulated a collection of $N = 20$ vortices each with a piecewise-linear representation with $M = 1024$ segments and ran the system to equilibration, determined by the settling of the mean and variance of the total energy. We ran the system for 20 logarithmically spaced values of β between 0.001 and 1 plus two points, 10 and 100. We set $\alpha = 10^7$ (enforcing straightness), $\mu = 2000$, and $L = 10$. Decreasing β simulates an increase in temperature, $1/\beta$. Units are arbitrary, with those chosen for α and β (e.g. ergs per centimeter and inverse ergs) determining those of R (e.g. centimeters) or vice versa. We calculate two arithmetic averages: the mean square vortex position,

$$R_{\text{MC}}^2 = (MN)^{-1} \sum_{i=1}^{N} \sum_{k=1}^{M} |\psi_i(k)|^2, \quad (31)$$

and the mean square amplitude per segment,

$$a^2 = (MN)^{-1} \sum_{i=1}^{N} \sum_{k=1}^{M} |\psi_i(k) - \psi_i(k+1)|^2, \quad (32)$$

where $\psi_i(M+1) = \psi_i(1)$.

Measures of the Monte Carlo R_{MC}^2, (31), correspond well to the 3D R^2, (26), in Fig. 4, whereas the strictly 2D R_{2D}^2, (9), continues to decline when the others curve up with decreasing β values, suggesting that the 3D effects are not only real in the Monte Carlo simulation but that the mean field is a good approximation with these parameters.

https://doi.org/10.1017/S0022377809008137 Published online by Cambridge University Press

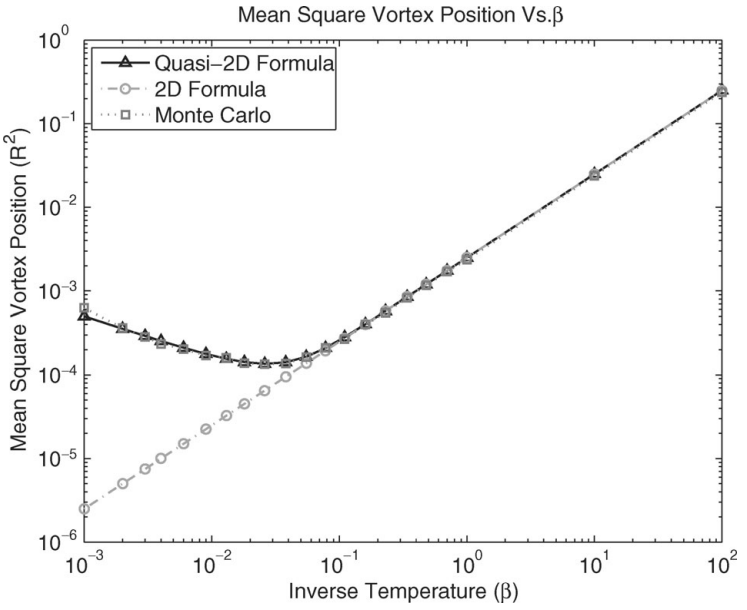

Figure 4. The mean square vortex position, defined in (31), compared with (26) and (9) shows how 3D effects come into play around $\beta = 0.16$. That, in the 2D formula, R^2_{2D} continues to decrease while the Monte Carlo and the quasi-2D radii curve upwards with decreasing β suggests that the internal variations of the vortex lines have a significant effect on the probability distribution of vortices.

6.2. Straightness holds

In order to be considered straight enough, we need

$$a \ll \frac{L}{M} = \frac{10}{1024} \sim 0.0098. \tag{33}$$

Straightness holds for all β values, shown in Fig. 5. These conditions hold on average. We ignore extreme low-probability cases as not contributing significantly to the statistics. Because of these straightness constraints, coupled with filaments having no attractive interactions, hairpins (kinks or, in quantum terminology, instantons) do not occur.

Aside from straightness constraints, the reader might question whether allowing vortex filaments to entangle violates the model's assumptions. While this is a valid concern, it is not an assumption of the model. Since this fluid is almost-everywhere inviscid, it contains asymptotically small regions of non-zero viscosity and, while a totally inviscid fluid cannot allow vortices to change topology (cross over each other) from state to state, an almost-everywhere inviscid fluid allows vortex reconnections and crossovers to occur due to microscopic viscous effects. Therefore, in our simulations vortices are allowed to cross one another. We are not claiming to model vortex reconnection, which is a mysterious process, but only the before and after effects of it.

Concerning the question of how vortices can cross one another and still remain nearly parallel, we point to the extremely high density (tiny value of R^2), which allows even the straightest filaments to entangle.

https://doi.org/10.1017/S0022377809008137 Published online by Cambridge University Press

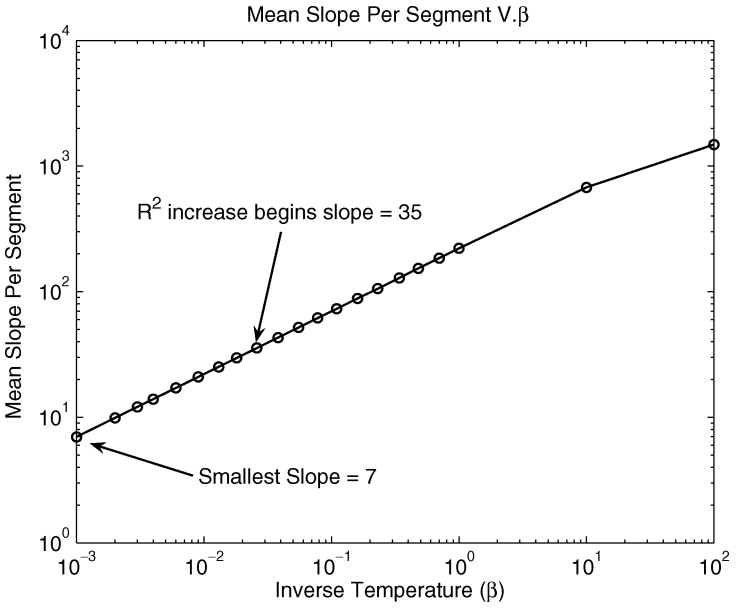

Figure 5. This figure shows the mean slope per segment, ϵ/a, where $\epsilon \sim 0.0098$ and a is given by (32), and that straightness holds for all β values. The point at which R^2 begins to increase with decreasing β (Fig. 4) has a mean slope of 35 and, even at the smallest $\beta = 10^{-3}$, the segments have an average angle of 82° with respect to the complex plane.

7. Conclusion

The decreasing-β, R-expansion suggests that, by adding degrees of freedom to the 2D model to make it a quasi-2D model, we add a mechanism for the vortices to resist confinement through entropic effects. As β decreases past the transition, the system's R^2 goes from being the result of interaction-versus-angular momentum competition to an entropy-versus-angular momentum competition. In the 2D system this third-dimension entropy is not there. Although there is another kind of entropy in the 2D model that will slow the compression as $\beta \to 0$ to a constant value, it is not enough to cause an increase in the system size. In the 3D system, the degrees of freedom are exponentially greater, which causes the expansion seen in Fig. 4.

The explicit formula for the length scale provides a way to quickly explore the parameter space of the statistical system and find areas of interest for a more in-depth study, and to determine hard to measure parameters, such as α and β, from the system size, R. The periodic geometry we are using applies to very large tori as well as columns. Therefore, these results can apply to a tokamak as well as stellar atmospheres. The expansion of the system shows that tight confinement of plasma columns is much more difficult when 3D effects are taken into account than a 2D system implies. However, non-uniformities in the distribution of filaments may allow tighter confinement towards the core than in the periphery of the system. Such a possibility has been suggested by Kiessling and Neukirch [31] and in our earlier paper on the microcanonical ensemble [21]. Therefore, further research on the density distribution is called for.

https://doi.org/10.1017/S0022377809008137 Published online by Cambridge University Press

Acknowledgements

This work is supported by ARO grant W911NF-05-1-0001 and DOE grant DE-FG02-04ER25616.

Appendix A. Proof of formula for R^2

The theorem follows from a steepest descent argument. In employing steepest descent, we need to start with an integral of the form $\int dx\, e^{-MF[x]}$. Then, if $F[x_0] < F[x]$ for all $x \neq x_0$, i.e. its minimum value is at x_0,

$$\lim_{M\to\infty} M^{-1} \log\left(\int dx\, e^{-MF[x]}\right) = F[x_0].$$

This works because, as M increases, the distribution that $e^{-MF[x]}$ represents becomes narrower and focuses on x_0 until the distribution has zero value at all other x.

Let us assume that N is large and take the limit over M first. We can pull the constant terms out of the integral of $Z'_N(M)$ over Ψ. Because F is positive definite, under Fubini's theorem we may switch the integrals to obtain

$$Z'_N(M) = e^{N^2\beta L/4 \log R^2 - \mu N L R^2} \int_{-\infty}^{\infty} \frac{d\sigma}{2\pi} \int d\Psi\, e^{-NF'[i\sigma]}, \tag{A 1}$$

where

$$F'[i\sigma] = \alpha\beta \sum_{k=1}^{M} \frac{1}{2} \frac{|\psi(k+1) - \psi(k)|^2}{\epsilon} + i\sigma\left(\sum_{k=1}^{M} |\psi(k)|^2 - MR^2\right) \tag{A 2}$$

is the part of the free energy still dependent on Ψ.

The interior integral needs evaluation. Let $s = i\sigma$ and define a new partition function

$$Z'(M) = \int_{-i\infty}^{i\infty} \frac{ds}{2\pi} \int d\Psi\, e^{-F'[s]}, \tag{A 3}$$

be that interior. Let us put F' in matrix form:

$$F'[s] = -sMR^2 + K\Psi^\dagger A\Psi + s\Psi^\dagger\Psi, \tag{A 4}$$

where $K = \alpha\beta/\epsilon$ and the $M \times M$ matrix A has the form

$$A_{i,i} = 1,$$

$$A_{i,i+1} = A_{i+1,i} = A_{1,M} = A_{M,1} = -\frac{1}{2},$$

$$A_{i,j} = 0, \quad \text{other } i, j.$$

The integral in (A 3) is Gaussian. We can evaluate it, knowing the eigenvalues of the matrix A. These eigenvalues have the form $\lambda_i = 1 - \cos(2\pi(i-1)/M)$ (not related to the previous use of λ_i as strength of vorticity) [23, 27], and so

$$Z'(M) = \int_{-i\infty}^{i\infty} \frac{ds}{2\pi} e^{sMR^2} \pi^M \prod_i \frac{1}{s + K\lambda_i}. \tag{A 5}$$

https://doi.org/10.1017/S0022377809008137 Published online by Cambridge University Press

We need to put $Z'(M)$ back into the correct form for steepest descent. Following the example of Berlin and Kac, let $s = K(\eta - 1)$; then

$$Z'(M) = \int_{-i\infty}^{i\infty} \frac{d\eta}{2\pi} K\pi^M (\eta - 1)^{-1} e^{-M \log(K)} e^{M f[\eta]}, \tag{A 6}$$

where

$$f[\eta] = KR^2(\eta - 1) - M^{-1} \sum_{i=2}^{M} \log(\eta - \cos(2\pi(i-1)/M)) \tag{A 7}$$

and $\eta \geqslant 1$.

We leave the $i = 1$ term out of the sum in $f[\eta]$ so that we can evaluate f further by taking the limit on the second term,

$$\lim_{M\to\infty} M^{-1} \sum_{i=2}^{M} \log(\eta - \cos(2\pi(i-1)/M)) = \frac{1}{2\pi} \int_0^{2\pi} d\omega \, \log(\eta - \cos(\omega)),$$

which gives

$$\begin{aligned} f[\eta] &= KR^2(\eta - 1) - \frac{1}{2\pi} \int_0^{2\pi} d\omega \log(\eta - \cos(\omega)) \\ &= KR^2(\eta - 1) - \log(\eta + (\eta^2 - 1)^{1/2}). \end{aligned} \tag{A 8}$$

To apply steepest descent, we determine the saddle point $\eta = \eta_0$ where $f[\eta]$ has its minimum value, $f[\eta_0]$. Taking the derivative and setting it equal to zero,

$$\frac{\partial f}{\partial \eta} = KR^2 - \frac{1}{\sqrt{\eta^2 - 1}} = 0, \tag{A 9}$$

implying that

$$\eta_0 = \sqrt{\frac{1}{(KR^2)^2} + 1}. \tag{A 10}$$

Having evaluated f, we can give an equation for the original free energy. Letting $N\beta \to \beta'$ and $\alpha/N \to \alpha'$,

$$F[\eta_0] = -\beta' L/4 \log R^2 + \mu L R^2 + M \log(K) - M f[\eta_0], \tag{A 11}$$

and evaluate it as $M \to \infty$. We will drop primes on β and α in the following.

The term in the limit $M \log(K)$ does not depend on R^2, and it is an unnecessary component representing the entropy of the broken filaments in the non-interacting case, and we drop it. Now we fill in the expressions for η_0 and K as defined above:

$$\begin{aligned} &\lim_{M\to\infty} M f[\eta_0] \\ &\quad = \lim_{M\to\infty} KR^2(\eta_0 - 1) - M \log(\eta_0 + (\eta_0^2 - 1)^{1/2}) \\ &\quad = \lim_{M\to\infty} MKR^2 \left(\sqrt{\frac{1}{(KR^2)^2} + 1} - 1 \right) - M \log\left(\sqrt{\frac{1}{(KR^2)^2} + 1} + \frac{1}{KR^2} \right) \end{aligned}$$

https://doi.org/10.1017/S0022377809008137 Published online by Cambridge University Press

$$= \lim_{M\to\infty} M\frac{\alpha\beta M}{L}R^2\left(\sqrt{\frac{1}{((\alpha\beta M/L)R^2)^2}+1}-1\right)$$

$$-M\log\left(\sqrt{\frac{1}{((\alpha\beta M/L)R^2)^2}+1}+\frac{1}{(\alpha\beta M/L)R^2}\right), \tag{A 12}$$

which, because it is an energy for a filament, ought to be finite. The first term is the energy of the filament, $E_{\rm fil}$, and the second, the entropy, $S_{\rm fil}$, and each by itself is finite, so we take each limit separately:

(i) the energy:

$$E_{\rm fil} = \lim_{M\to\infty} M\frac{\alpha\beta M}{L}R^2\left(\sqrt{\frac{L^2}{(\alpha\beta M R^2)^2}+1}-1\right) = \frac{L}{2\alpha\beta R^2}. \tag{A 13}$$

(ii) the entropy:

$$S_{\rm fil} = \lim_{M\to\infty} M\log\left(\sqrt{\frac{1}{((\alpha\beta M/L)R^2)^2}+1}+\frac{1}{(\alpha\beta M/L)R^2}\right) = \frac{L}{\alpha\beta R^2}. \tag{A 14}$$

These two results imply that

$$\lim_{M\to\infty} Mf[\eta_0] = -\frac{L}{2\alpha\beta R^2}$$

and

$$F[\eta_0] = L\mu R^2 - \beta L/4\log R^2 + \frac{L}{2\alpha\beta R^2}. \tag{A 15}$$

We minimize with respect to R^2,

$$\frac{\partial F}{\partial R^2} = L\mu - \frac{\beta L}{4R^2} - \frac{L}{2\alpha\beta R^4} = 0, \tag{A 16}$$

and solve for R^2,

$$R^2 = \frac{\beta/4 \pm \sqrt{(\beta/4)^2 + 4\mu(1/2\alpha\beta)}}{2\mu}$$

$$= \frac{\beta^2\alpha + \sqrt{\beta^4\alpha^2 + 32\alpha\beta\mu}}{8\alpha\beta\mu}, \tag{A 17}$$

where we take the 'plus' solution as giving physical results.

References

[1] Onsager, L. 1949 Statistical hydrodynamics. *Nuovo Cimento Suppl.* **6**, 279–287.

[2] Joyce, G. R. and Montgomery, D. 1973 Negative temperature states for a two-dimensional guiding center plasma. *J. Plasma Phys.* **10**, 107.

[3] Edwards, S. F. and Taylor, J. B. 1974 Negative temperature states for two-dimensional plasmas and vortex fluids. *Proc. R. Soc. Lond.* A. **336**, 257–271.

[4] Caglioti, E., Lions, P. L., Marchioro, C. and Pulvirenti, M. 1992 A special class of stationary flows for two-dimensional Euler equations: a statistical mechanics description. *Commun. Math. Phys.* **143**, 501–525.

[5] Kiessling, M. 1993 Statistical mechanics of classical particles with log interactions. *Commun. Pure Appl. Math.* **46**, 27–56.

https://doi.org/10.1017/S0022377809008137 Published online by Cambridge University Press

[6] Kiessling, M. and Spohn, H. 2001 A note on the eigenvalue density of random matrices. *Commun. Math. Phys.* **199**, 683–695.

[7] Lim, C. C. 2005 Recent advances in 2d and 2.5d vortex statistics and dynamics. In: *Proc. 35th American Institute of Aeronautics and Astronautics Fluid Dynamics Conf., Toronto, Canada* (paper no. 2005–5158).

[8] Lim, C. C. and Nebus, J. 2006 *Vorticity Statistical Mechanics and Monte Carlo Simulations*. New York: Springer.

[9] Hasimoto, H. 1972 A soliton on a vortex filament. *J. Fluid Mech.* **51**, 472.

[10] Callegari, A. J. and Ting, L. 1978 Motion of a curved vortex filament with decaying vortical core and axial velocity. *SIAM J. Appl. Math.* **35**(1), 148–175.

[11] Klein, R. and Majda, A. J. 1991 Self-stretching of a perturbed vortex filament I: the asymptotic equation for deviations from a straight line. *Physica* D **49**, 323.

[12] Ting, L. and Klein, R. 1991 *Viscous Vortical Flows (Lecture Notes in Physics, 374)*. Berlin: Springer.

[13] Uby, L., Isichenko, M. B. and Yankov, V. V. 1995 Vortex filament dynamics in plasmas and superconductors. *Phys. Rev.* E **52**, 932–939.

[14] Kinney, R., Tajima, T. and Petviashvili, N. 1993 Discrete vortex representation of magnetohydrodynamics. *Phys. Rev. Lett.* **71**, 1712–1715.

[15] Klein, R., Majda, A. and Damodaran, K. 1995 Simplified equation for the interaction of nearly parallel vortex filaments. *J. Fluid Mech.* **288**, 201–248.

[16] Weinan, E. 1994 Dynamics of vortex liquids in Ginsburg–Landau theories with applications to superconductivity. *Phys. Rev.* B **50**(2), 1126–1135.

[17] Gordeev, A. V., Kingsep, A. S. and Rudakov, L. I. 1994 Electron magnetohydrodynamics. *Phys. Rep.* **243**, 215.

[18] Molenaar, D., Clercx, H. and van Heijst, G. 2005 Transition to chaos in a confined two-dimensional fluid flow. *Phys. Rev. Lett.* **95**, 104503.

[19] Chorin, A. J. 1994 *Vorticity and Turbulence*. New York: Springer.

[20] Haken, H. 1975 Cooperative phenomena in systems far from thermal equilibrium and in nonphysical systems. *Rev. Mod. Phys.* **47**(1), 67–121.

[21] Andersen, T. D. and Lim, C. C. 2007 Negative specific heat in generalized quasi-2d vorticity. *Phys. Rev. Lett.* **99**, 165001.

[22] Lim, C. C. and Assad, S. M. 2005 Self-containment radius for rotating planar flows, single-signed vortex gas and electron plasma. *Regul. Chaot. Dyn.* **10**, 240–254.

[23] Lions, P.-L. and Majda, A. J. 2000 Equilibrium statistical theory for nearly parallel vortex filaments. *Commun. Pure Appl. Math.* **53**, 76–142.

[24] Abrikosov, A. A. 1957 On the magnetic properties of superconductors of the second group. *Sov. Phys. JETP* **5**(6), 1442–1452.

[25] Ivonin, I. A. 1992 Stability of two-dimensional vortices against three-dimensional perturbations in a fluid and in electron hydrodynamics. *Sov. J. Plasma Phys.* **18**, 302.

[26] Assad, S. M. and Lim, C. C. 2005 Statistical equilibrium of the coulomb/vortex gas in the unbounded two-dimensional plane. *Discrete Contin. Dyn. Syst.* B **5**(1), 1–14.

[27] Berlin, T. H. and Kac, M. 1952 The spherical model of a ferromagnet. *Phys. Rev.* **86**(6), 821.

[28] Zee, A. 2003 *Quantum Field Theory in a Nutshell*. Princeton: Princeton University Press.

[29] Feynman, R. P. and Wheeler, J. W. 1948 Space–time approach to non-relativistic quantum mechanics. *Rev. Mod. Phys.* **20**, 367.

[30] Ceperley, D. M. 1995 Path integrals in the theory of condensed helium. *Rev. Mod. Phys.* **67**, 279.

[31] Kiessling, M. K.-H. and Neukirch, T. 2003 Negative specific heat of a magnetically self-confined plasma torus. *Proc. Natl. Acad. Sci. USA* **100**, 1510–1514.